ELSEVIER

Journal of Nuclear Materials 304 (2002) 56–62

journal of nuclear materials

www.elsevier.com/locate/jnucmat

Crystal chemistry of uranium (V) and plutonium (IV) in a titanate ceramic for disposition of surplus fissile material ☆

J.A. Fortner *, A.J. Kropf, R.J. Finch, A.J. Bakel, M.C. Hash, D.B. Chamberlain

Chemical Technology Division, Argonne National Laboratory, 9700 South Cass Avenue, Argonne, IL 60439-4837, USA

Received 10 December 2001; accepted 9 April 2002

Abstract

We report X-ray absorption near-edge structure (XANES) and extended X-ray absorption fine-structure (EXAFS) spectra for the plutonium LIII and uranium LIII edges in titanate pyrochlore ceramic. The titanate ceramics studied are of the type proposed to serve as a matrix for the immobilization of surplus fissile materials. The samples studied contain approximately 10 wt% fissile plutonium and 20 wt% natural uranium, and are representative of material within the planned production envelope. Based upon natural analogue models, it had been previously assumed that both uranium and plutonium would occupy the calcium site in the pyrochlore crystal structure. While the XANES and EXAFS signals from the plutonium LIII are consistent with this substitution into the calcium site within pyrochlore, the uranium XANES is characteristic of pentavalent uranium. Furthermore, the EXAFS signal from the uranium has a distinct oxygen coordination shell at 2.07 Å and a total oxygen coordination of about 6, which is inconsistent with the calcium site. These combined EXAFS and XANES results provide the first evidence of substantial pentavalent uranium in an octahedral site in pyrochlore. This may also explain the copious nucleation of rutile (TiO_2) precipitates commonly observed in these materials as uranium displaces titanium from the octahedral sites. © 2002 Published by Elsevier Science B.V.

PACS: 61.10.H; 61.66.F; 78.70.D

1. Introduction

The Department of Energy (DOE) is preparing to dispose of surplus and residual plutonium from nuclear disarmament and environmental remediation of weapons facilities. Some of this material may be slated for direct disposal in a proposed geologic repository at the Yucca Mountain site. Although small in volume and total radioactivity compared to other materials planned for disposal in the repository, the highly loaded (~10 wt% plutonium) waste form will create unique concerns, including the potential for criticality. Criticality is addressed by adding the neutron-absorbing elements hafnium and gadolinium to the ceramic formulation, and by diluting the ^{235}U progeny by addition of depleted uranium. Owing to the many challenges in developing chemical and natural analog models for the long-term behavior of this material, a thorough physical, mineralogical, and chemical characterization is needed. We demonstrate the efficacy of X-ray absorption spectroscopy near-edge spectroscopy (XANES) and extended X-ray absorption fine-structure (EXAFS) analyses to characterize the oxidation states and coordination environments of plutonium and uranium in prototype specimens of this ceramic.

☆ This work was supported by the US Department of Energy Office of Fissile Materials Disposition under Contract no. W-31-109-Eng-38. Use of the Advanced Photon Source was supported by the US Department of Energy, Basic Energy Sciences, Office of Energy Research (DOE-BES-OER), under Contract no. W-31-109-Eng-38. The MRCAT beamlines are supported by the member institutions and the US DOE-BES-OER under contracts DE-FG02-94ER45525 and DE-FG02-96ER45589.

* Corresponding author. Tel.: +1-630 252 5594; fax: +1-630 972 4438.

E-mail address: fortner@cmt.anl.gov (J.A. Fortner).

0022-3115/02/$ - see front matter © 2002 Published by Elsevier Science B.V.
PII: S0022-3115(02)00870-X

2. Experimental method

Two formulations of the ceramic were examined, representing pure and impure feedstocks of the fissile material. The chemical formulations of the baseline (A0) and high-impurity (A9) titanate ceramics studied are provided in Table 1. The starting materials for the samples were calcined in static air at 750 °C. The resulting powders were then cold pressed and sintered in flowing argon at 1350 °C for ~4 h. Based upon SEM and X-ray diffraction data, the major phases in these ceramics are pyrochlore [$A_2B_2O_7$], zirconolite [$AA'B_2O_7$], Hf-bearing rutile [$(Hf,Ti)O_2$], and brannerite [$(U,Pu)Ti_2O_6$], where A = Ca, actinides (ACT), and rare earth elements (REE); A′ = Zr, REE, and Hf; and B = ACT, REE, Ti Zr, and Hf [1,2]. Pyrochlore (with included zirconolite) accounts for approximately 70–80% of the ceramic volume in both the A0 and A9 formulations. Up to 20% of the volume may be brannerite. Much of the remaining volume (up to 10% of the total) is composed of rutile. Thus, the majority of the U and Pu is contained within the pyrochlore/zirconolite phase in each formulation.

Pyrochlore is structurally related to zirconolite, being essentially a cubic polytype. The cations in pyrochlore may be $A^{3+}B^{4+}$, $A^{2+}B^{5+}$, or some other combination that may include vacancies [3,4]. More generally, pyrochlore can have the formula $A_{2-x}B_2O_6Y_m$, where the ideal cubic structure has $x = 0$ and $m = 1$ (Fig. 1). Typically, the Y site is occupied by O, OH, F, etc., allowing various charge-compensation arrangements with the A site. This variety of possible coupled substitutions in pyrochlore contributes to its attractiveness as a ceramic waste form. A recent transmission electron microscopy study of the detailed phase assemblage in one of the prototype immobilization ceramics has shown that zirconolite inclusions grow epitaxially as lamellae within the pyrochlore phase [5]. Additional minor phases may occur depending on waste loading; these include uranium oxides and glassy phases [1,2,5]. The glassy phases and rutile fill interstices between the major phases. Both Hf and Gd are added to the ceramic formulation as neutron absorbers in order to satisfy a defense-in-depth concept for the waste form. Also in Table 1 is the expected single-phase formula of each ceramic. The formulae at the bottom of Table 1 assume that each ceramic is 100% pyrochlore, and that only Ti completely occupies the 'B' site; as we shall see, this is likely contrary to the actual structure.

The EXAFS measurements were made at the undulator beam line of the Materials Research Collaborative Access Team (MRCAT) at Argonne National Laboratory. Measurements were made in fluorescence mode with the incident intensity ionization chamber optimized

Table 1
Ceramic compositions in weight percent

Compound	Specimen Type	
	A0	A9
CaO	9.95	9.44
TiO_2	35.87	34.04
HfO_2	10.65	10.11
Gd_2O_3	7.95	7.54
UO_2	23.69	22.48
PuO_2	11.89	11.28
Al_2O_3	–	0.50
MgO	–	0.44
$CaCl_2$	–	0.66
Ga_2O_3	–	0.57
Fe_2O_3	–	0.15
Cr_2O_3	–	0.08
NiO	–	0.13
CaF_2	–	0.44
K_2O	–	0.32
Na_2O	–	0.14
MoO_2	–	0.28
SiO_2	–	0.46
Ta_2O_5	–	0.19
B_2O_3	–	0.17
WO_2	–	0.49
ZnO	–	0.07
Expected formula ($A_2Ti_2O_7$ basis)	$A_{1.87}Ti_{2.09}O_7$	$A_{2.11}Ti_{1.97}O_7$ $(F,Cl)_{0.106}$

A0 = 'baseline' ceramic, A9 = 'high impurity' ceramic.

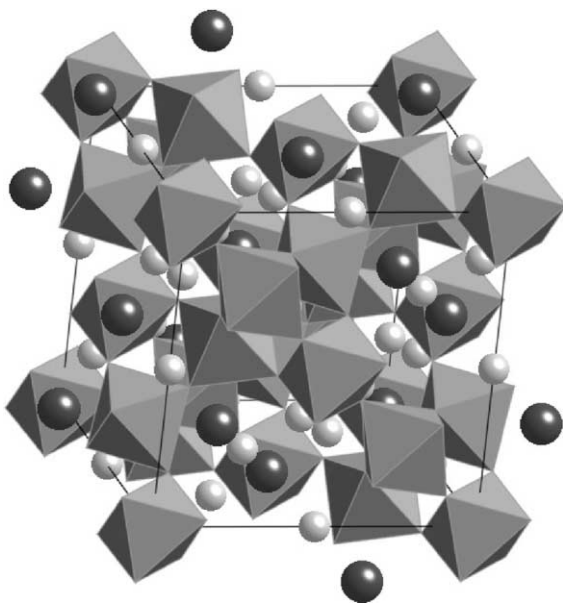

Fig. 1. Cubic pyrochlore structure illustrated using a polyhedral model, showing the corner-linked B-site octahedra. The A and Y sites are the small, light and large, dark spheres, respectively.

for maximum current with linear response ($\sim 10^{10}$ photons detected/s). The fluorescence ionization chamber was filled with xenon gas and produced a signal of $\sim 10^8$ photons/s above the absorption edge. A double-crystal Si(1 1 1) monochromator was used in conjunction with a Pt-coated mirror to minimize the presence of harmonics. The counting time at each measured wavelength ranged from 2 to 8 s per point in the EXAFS region. We used the program *feffit* from the University of Washington package to fit the spectra and *feff*, version 8.00, to calculate the X-ray scattering paths [6].

2.1. Plutonium coordination

An analysis of the XANES and EXAFS of the plutonium LIII edge in these ceramics has been published previously [7], where it was shown that the plutonium is predominately in the (IV) oxidation state. The EXAFS Fourier transform analysis shown in Fig. 2 demonstrates a coordination environment for plutonium in the ceramic that differs from PuO_2 in both the first (Pu–O) and second coordination shells [7,8]. The second shell coordination ($r = 3.59$ Å) environment from the EXAFS in the figure was fitted as due predominantly to titanium

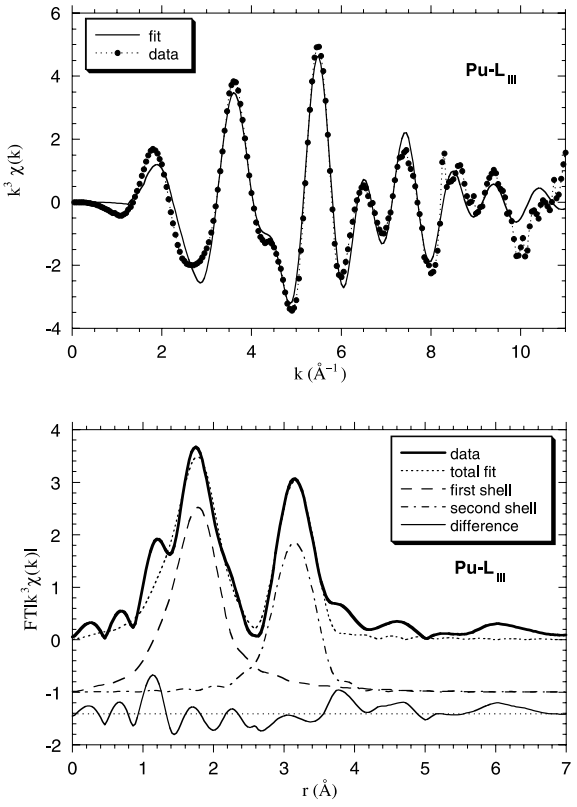

Fig. 2. Plutonium EXAFS (top) with Fourier transform moduli (bottom) with shell fits.

Table 2
Coordination results from and Pu-LIII EXAFS analysis

Sample	Atom pair	R (Å)	N	σ^2
A0	Pu–O	2.30 ± 0.05	10 ± 2	0.020 ± 0.004
	Pu–Ti	3.59 ± 0.02	9 ± 2	0.013 ± 0.004
A9	Pu–O	2.30 ± 0.05	10 ± 3	0.022 ± 0.004
	Pu–Ti	3.59 ± 0.02	13 ± 3	0.018 ± 0.004

R is the coordination distance, with coordination number N and Debye-Waller factor σ^2.

Table 3
Coordination in Nb(V) pyrochlore, adapted from [14]

Atom pair	R (Å)	N
Nb–O	1.99	6
Nb–nnn[a]	3.69	6 (Ca) and 6 (Nb)
Ca–O	2.26 (×2), 2.63 (×6)	8
Ca–nnn[a]	3.69	6 (Ca) and 6 (Nb)

[a] nnn = next nearest neighbor.

(Table 2). The structure is consistent with Pu occurring at the 'A' site in the structures of pyrochlore or zirconolite. This interpretation is affirmed by comparison with the coordination environment of Ca in $Ca_2Nb_2O_7$ pyrochlore (Table 3).

2.2. Uranium coordination

The U-LIII absorption edge reveals substantially different characteristics for the uranium environment from that of plutonium in this material (Fig. 3). The uranium EXAFS data were fitted using the *feff* 8 package over the k range of 3 to 10 Å^{-1} with k^3 weighting. The first coordination U–O shell was obtained at 2.05–2.07 Å, with a coordination number of about 3 for both the A0 and A9 samples (Table 4). This unusual U–O bond length does not match the short apical bonds of the uranyl ion (~1.85 Å) or the U(IV)–O bond length of around 2.4 Å. A clear second shell surrounds the uranium in both specimens at about 2.36 Å, also with a coordination of about 3. The third peak in the EXAFS Fourier transform was fitted assuming it originated from titanium, yielding a peak at 3.59 Å, a shell common to both A and B sites in pyrochlore (Tables 3 and 4).

2.3. Difference spectra: A0–A9

No significant difference appeared between the baseline (A0) and high-impurity (A9) ceramic formulations in the measured XANES and EXAFS of either uranium or plutonium. This strongly suggests that the titanium pyrochlore-based ceramic is robust as a waste form inasmuch as the crystal chemistry of the entrained acti-

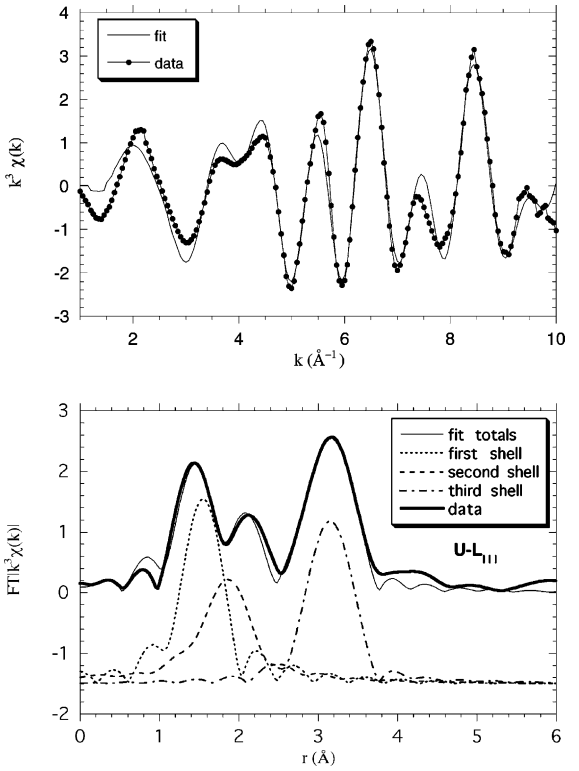

Fig. 3. Uranium EXAFS (top) with Fourier transform moduli (bottom) with shell fits. In comparison with Fig. 2, the uranium and plutonium have distinctly different coordination shells.

nides is insensitive to the presence of impurities in the feedstock (Table 1). This is consistent with extensive corrosion testing data, which indicate little impact of impurities on the release behavior of the actinides or neutron poisons (Gd and Hf) [1,2]. Nonetheless, small differences in the spectra were closely examined. We obtained difference spectra by a procedure that is described briefly below; more detail can be found in Miller et al. [9].

Table 4
Coordination results from and U-LIII EXAFS analysis

Sample	Atom pair	R (Å)	N	σ^2
A0	U–O(1)	2.07 ± 0.04	4 ± 1	0.009 ± 0.003
	U–O(2)	2.36 ± 0.06	3 ± 1	0.010 ± 0.005
	U–Ti	3.59 ± 0.02	9 ± 2	0.014 ± 0.004
A9	U–O(1)	2.05 ± 0.04	3 ± 1	0.007 ± 0.003
	U–O(2)	2.36 ± 0.06	3 ± 1	0.012 ± 0.005
	U–Ti	3.59 ± 0.02	8 ± 2	0.012 ± 0.005

Symbols labeled as in Table 2.

First, the uranium and plutonium absorption spectra from the A0 and A9 ceramics were normalized to the height of the absorption edge 'white line'. As a check, differences between consecutive runs of the A0 ceramic contained little structure, as expected. Difference curves (A0–A9) were obtained from both the uranium and plutonium spectra. Small adjustments (<0.05 eV) were made to the edge position of the A9 spectra to minimize a second-derivative contribution that would arise from misalignment of the spectral edges owing to instrumental drift. The resulting difference spectra, multiplied 10-fold, appear with the total spectra in Fig. 4. Interestingly, the difference spectra suggest a distinct actinide phase in the baseline ceramic (A0) that is absent in the

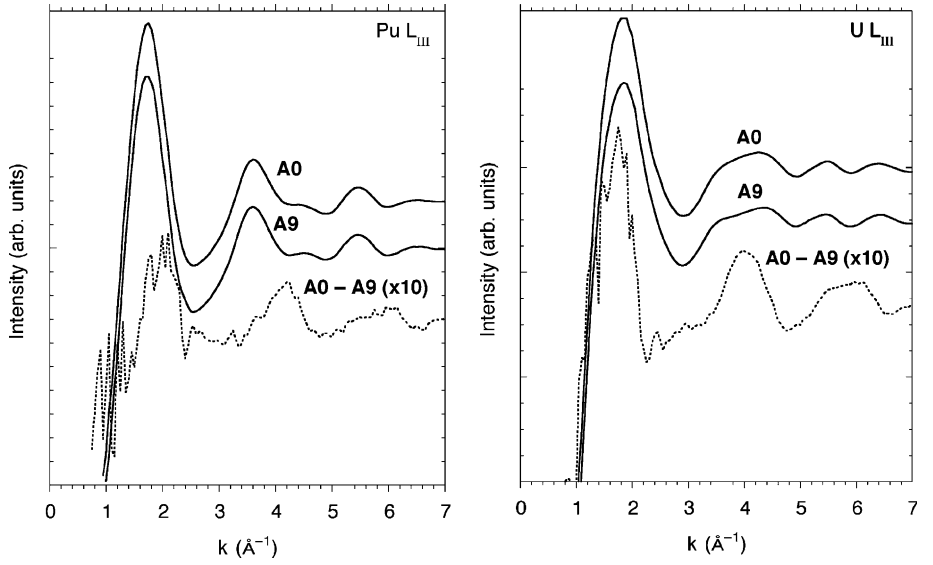

Fig. 4. EXAFS spectra of the two specimens, along with the difference signal (A0–A9) multiplied 10-fold. Left, Pu, and right, U.

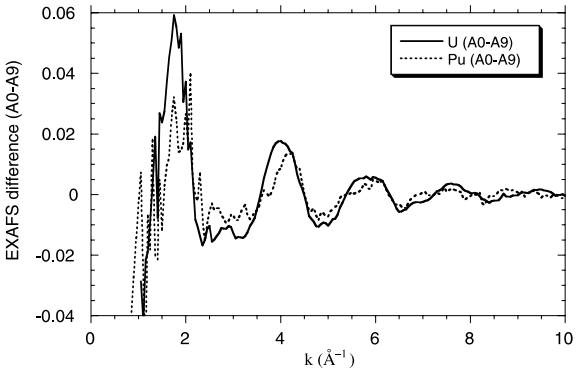

Fig. 5. The EXAFS difference signals (A0–A9) for uranium (solid line) and plutonium (dashed line) bear a striking simularity, suggesting similar crystallographic siting within a minor phase more common in A0 (likely brannerite).

impurity ceramic (A9). Prior scanning electron microscopy (SEM) of these ceramics indicates brannerite (nominally UTi_2O_6) as the likely phase responsible because it appeared that the impurities in the ceramic feed suppressed the growth of this phase [1,2]. The difference spectra from both the uranium and plutonium edges are compared directly with one another in Fig. 5. The similarity of the structure in these difference spectra indicates that uranium and plutonium occupy similar sites in the brannerite.

3. Discussion

A comparison of the uranium data with the plutonium coordination environment summarized in Table 2 strongly suggests that the uranium occupies a distinct crystallographic site from the plutonium in these specimens, since it differs in both oxygen bond length(s) and total coordination number in the first sphere. We note that the observed uranium coordination environment, particularly the presence of 2.05–2.07 Å bonds, is characteristic of pentavalent uranium [10]. A comparison with known U(V)–O bond lengths in other compounds (Table 5) supports our interpretation of pentavalent uranium in the pyrochlore.We acknowledge that distorted-octahedral coordination of U^{6+}, lacking the characteristic apical bonds of the uranyl ion, has been noted in several compounds [11]. However, according to the review by Burns et al. [11], distorted-octahedral U^{6+} has not been reported to have bond lengths of ~2.05 and ~2.36 Å *simultaneously*, as we observe for the titanate specimens in this study. From Table 3, the octahedral 'B' site in pyrochlore (e.g., Nb in $Ca_2Nb_2O_7$) would accommodate the smaller, lower coordination U^{5+} ion. From a charge-balance perspective, the B site is certainly a more logical site for pentavalent uranium. Pentavalent uranium is often overlooked as a possible valence state, owing to its rather small stability field in aqueous solution and consequential paucity in geologic minerals [10]. The specimens considered here, however, were not formed under aqueous conditions but by solid-state reaction, as described earlier. Nonetheless, it appears that previous assumptions of U(IV) occupying the A site in pyrochlore, as we observed for plutonium, are unsubstantiated; in fact, we are unaware of *any* study that directly demonstrates this in any pyrochlore sample.

Further evidence for the presence of pentavalent uranium in these specimens can be obtained by careful examination of the near-edge absorption structure. The XANES of pentavalent uranium has been described by Farges et al. [12] in a study of silicate glasses, which were characterized by UV-visible spectroscopy and EXAFS/XANES. The XANES signal from these ceramics (Fig. 6) bears the signature of U(V) when compared with other materials of known uranium valence. Owing to the difficulty in producing reliable standards, we have not simultaneously examined U(IV), U(V), and U(VI) reference materials for a quantitative measurement of edge position. Nonetheless, the Pu and U EXAFS and XANES clearly indicate that (i) uranium and plutonium occupy structurally distinct sites within the pyrochlore-based ceramic and (ii) a substantial portion of the uranium is pentavalent. This surprising result may have implications for assumptions commonly made regarding valence in uranium-bearing titanate and niobate minerals; we shall return to this topic in the discussion to follow.

Table 5
Uranium–oxygen coordination in known pentavalent uranium compounds and minerals (adapted from Burns and Finch [10])

Compound or mineral	U^{5+}–O(1) distance (Å)	N(1)	U^{5+}–O(2) distance (Å)	N(2)	Reference
Wyartite	2.07–2.14	4	2.44–2.48	3	Burns and Finch [10]
U_2MoO_8	2.06–2.18	4	2.36–2.73	3	Serezhkin et al. [16]
$USbO_3$	1.93–2.13	3	2.30–2.50	4	Dickens and Stuttard [17]
UVO_5	2.05–2.07	2	2.21–2.32	5	Dickens et al. [18]
$U_5O_{12}Cl$	2.06	2	2.25–2.54	5	Cordfunke et al. [19]

In each case, the pentavalent uranium site can be described as a pentagonal bipyramid polyhedra (f_7), having seven neighbors in the first coordination sphere [N(1) + N(2)].

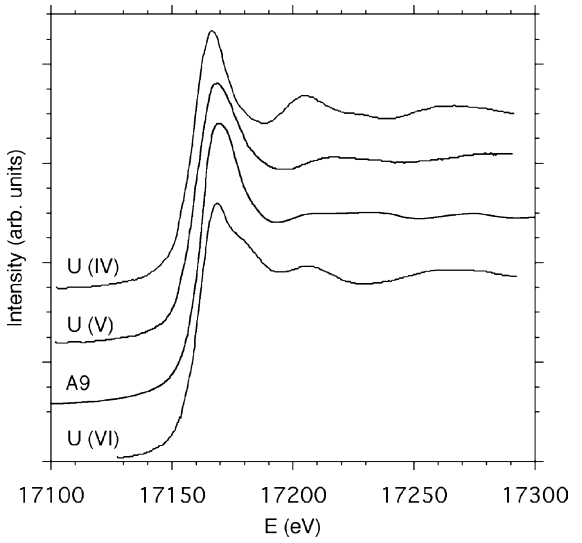

Fig. 6. Uranium XANES from the A9 ceramic with reference data from Farges et al. [12].

The presence of pentavalent uranium in the ceramic, which does *not* have the same local coordination as the plutonium, likely resides, at least in part, in the titanium (B) site of the pyrochlore phase. Comparison of Tables 3 and 4 suggests that at least half of the uranium (based upon the experimental coordination number fit) is located in a niobium site in the pyrochlore. It is worth noting that uranium displacing titanium from the B site may explain the relatively abundant rutile (up to ~20% by volume) that precipitates in the ceramic during fabrication, in excess of that expected from the assumed $A_2Ti_2O_7$ structure [1,2,5]. The starting compositions in Table 1 result in charge-neutral formulae, assuming plutonium and uranium are both in the +4 oxidation state. The precipitation of rutile in the final ceramic, however, would leave a deficit of charge in the pyrochlore, assuming the 7-oxygen ($A_2B_2O_7$) basis. Removal of only 5% of the titanium to form rutile can be completely charge compensated by pentavalent uranium, without the need to postulate oxygen vacancies. Finally, we note that the strong depletion of uranium in the zirconolite lamellar zones within pyrochlore observed by Buck et al. [5] suggests a substantial crystal chemical distinction between the preferred sites in these two phases. In pyrochlore, the octahedral B sites are fully corner linked, whereas in zirconolite, the Ti octahedra are corner linked only within sheets that do not crosslink. There is little to distinguish the A sites in pyrochlore from zirconolite, making uranium segregation between them unlikely. The zirconolite A′ site, which has no correspondant in pyrochlore, can readily accomodate several uranium ions [13], yet appeared less favorable during formation of these materials than the pyrochlore sites.

Pentavalent ions in titanium sites of pyrochlores and zirconolite are not uncommon. Indeed, the review by Subramanian et al. [3] places U^{5+} in the pyrochlore B site. Certain end members of Nb^{5+} pyrochlore have been found in nature and synthesized in the laboratory [14]. Diffuse reflectance spectroscopy has shown that zirconolites in SYNROC contain some fraction of uranium as U^{5+} [15]. An analysis of the coupled substitutions required to introduce 5+ ions to a titanium site in zirconolite is given by Gieré et al. [13]. However, previous analyses, including that of Gieré et al., have explicitly assumed that uranium in zirconolite would be quadravalent, residing in the calcium site. This assumption has frequently carried over to analyses of pyrochlores. Our observations indicate that such assumptions regarding uranium valence and site occupancy may need to be re-evaluated. To date, only one natural mineral (wyartite) is reported to contain U(V) as an essential constituent [10]. The present work shows that uranium-containing pyrochlores formed in an oxidizing environment are likely candidates to have incorporated pentavalent uranium.

Acknowledgements

This work was supported by the US Department of Energy Office of Fissile Materials Disposition. Use of the Advanced Photon Source was supported by the US Department of Energy, Basic Energy Sciences, Office of Energy Research (DOE-BES-OER), under Contract no. W-31-109-Eng-38. Work performed at MRCAT is supported, in part, by funding from the Department of Energy under grant number DEFG0200ER45811. The authors also thank Scott Aase and Don Reed of Argonne for valuable assistance with sample preparation and beamline operations, Allen Bakel and Edgar Buck of Argonne and E.R. 'Lou' Vance of ANSTO for useful discussions of the ceramic microstructure, and Henry Shaw (Lawrence Livermore) for encouraging the pursuit of this work.

References

[1] A.J. Bakel, V. Zyryanov, C.J. Mertz, E.C. Buck, D.B. Chamberlain, Mater. Res. Soc. Symp. Proc. 556 (1999) 181.
[2] A.J. Bakel, C.J. Mertz, E.C. Buck, S.F. Wolf, M.K. Nole, J.K. Basco, M.C. Hash, D.B. Chamberlain, Lawrence Livermore National Laboratory Report PIP-00-120, 2000.
[3] M.A. Subramanian, G. Aaravamundan, G.V. Subba Rao, Prog. Solid State Chem. 15 (1983) 55.
[4] D.D. Hogarth, Am. Mineral. 62 (1977) 403.
[5] E.C. Buck, D.B. Chamberlain, R. Gieré, Mater. Res. Soc. Proc. 556 (1999) 19.

[6] A.L. Ankudinov, B. Ravel, J.J. Rehr, S.D. Conradson, Phys. Rev. B 58 (1998) 7565;
E.A. Stern, M. Newville, B. Ravel, Y. Yacoby, D. Haskel, Physica B 208&209 (1995) 117.
[7] J.A. Fortner, A.J. Kropf, A.J. Bakel, M.C. Hash, S.B. Aase, E.C. Buck, D.B. Chamberlain, Mater. Res. Soc. Proc. 608 (2000) 401.
[8] S.R. Conradson, App. Spectros. 52 (7) (1998) 252A;
L.R. Morss, C.J. Mertz, A.J. Kropf, J.L. Holly, Mater. Res. Soc. Symp. Proc. 713 (2002) in press.
[9] J.T. Miller, C.L. Marshall, A.J. Kropf, J. Catal. 202 (2002) 89.
[10] P.C. Burns, R.J. Finch, Am. Mineral. 84 (1999) 1456.
[11] P.C. Burns, R.C. Ewing, F.C. Hawthorne, Can. Mineral. 35 (1997) 1551.
[12] F. Farges, C.W. Ponader, G. Calas, G.E. Brown Jr., Geochim. Cosmochim. Acta 56 (1992) 4205.
[13] R. Gieré, C.T. Williams, G.R. Lumpkin, Schweiz. Mineral. Petrogr. Mitt. 78 (1998) 433.
[14] J.T. Lewandowski, I.J. Pickering, A.J. Jacobson, Mater. Res. Bull. 27 (1992) 981.
[15] E.R. Vance, Australian Nuclear Science and Technology Organization (ANSTO), private communication.
[16] V.N. Serezhkin, L.M. Kovba, V.K. Trunov, Kristallographiya 18 (1973) 514.
[17] P.G. Dickens, G.P. Stuttard, J. Mater. Chem. 2 (1992) 691.
[18] P.G. Dickens, G.P. Stuttard, R.G.J. Ball, A.V. Powell, S. Hull, S. Patat, J. Mater. Chem. 2 (1992) 161.
[19] E.H.P. Cordfunke, P.V. Van Vlaanderen, K. Goubitz, B.O. Loopstra, J. Solid State Chem. 56 (1985) 166.